

Water Oxidation by Cobalt Centers on Various Oxide Surfaces: The Effects of Oxide Surface Acidity and Oxygen Atom Affinity on Catalysis

Hyun S. Ahn,^{†,‡,§} Junko Yano,^{||} and T. Don Tilley^{*,†,‡,§}

[†]Department of Chemistry, University of California, Berkeley, Berkeley, California 94720, United States

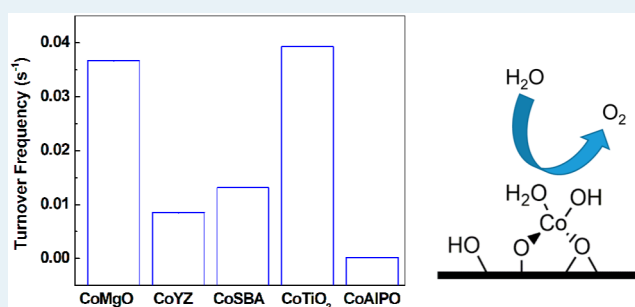
[§]Chemical Sciences Division, Lawrence Berkeley National Laboratory, 1 Cyclotron Road, Berkeley, California 94720, United States

^{||}Physical Biosciences Division, Lawrence Berkeley National Laboratory, 1 Cyclotron Road, Berkeley, California 94720, United States

Supporting Information

ABSTRACT: Single-atom cobalt centers on various oxide surfaces (TiO₂, MgO, SBA-15, AlPO, and Y-Zeolite) were prepared and evaluated as water oxidation catalysts by photochemical water oxidation experiments. Superior catalytic rates were observed for cobalt sites on basic supporting oxides (TiO₂ and MgO) relative to those on acidic oxides (Y-Zeolite, AlPO, and SiO₂). Per-atom turnover frequencies of ca. 0.04 s⁻¹ were achieved, giving initial rates 100 times greater than that of a surface atom of a Co₃O₄ nanoparticle. Contrary to expectations based on theoretical work, no apparent correlation was observed between the catalytic rates and the oxygen atom affinities of the supporting oxides.

KEYWORDS: water oxidation, oxide, single-site, cobalt, surface acidity, oxygen atom affinity

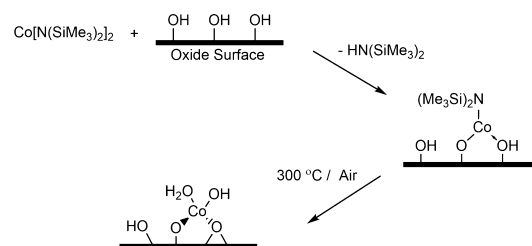


Achievement of artificial photosynthesis in a robust and economically viable device is an important technical challenge.¹ One significant hurdle is the development of efficient water oxidation catalysts, especially those employing only first-row, earth-abundant transition metals.^{2–4} As a result, the mechanisms of existing water oxidation catalysts have been studied in great detail to identify bottlenecks^{5,6} and elucidate structural requirements.⁷ However, many of the proposed mechanisms remain speculative. We recently reported the synthesis and evaluation of small-domain cobalt catalysts on SBA-15 silica and found that single-atom cobalt is not only active for water oxidation catalysis but also exhibits a higher turnover frequency (TOF) than that of a surface cobalt atom of Co₃O₄.⁷ Meyer and co-workers also found that single-atom cobalt on an FTO surface catalyzes electrochemical water oxidation.⁸ In addition, recent theoretical work suggests that the lowest-energy pathway for oxygen evolution on a multiatom cobalt oxide cluster involves geminal coupling of a cobalt-oxo with a hydroxyl or an aquo ligand.⁹ A similar pathway may be viable for a single-cobalt site of a heteroatom oxide support, and the properties of the supporting oxides such as surface basicity and oxygen atom affinity may govern the rate of catalysis.^{7,9} Herein we report the syntheses of single cobalt sites on a variety of oxide surfaces (MgO, TiO₂, AlPO, SBA-15, and Y-Zeolite), and evaluations of their abilities to catalyze water oxidation. Notably, single cobalt sites supported on basic supporting oxides (TiO₂ and MgO) exhibited superior catalysis relative to those on acidic oxides (Y-Zeolite, AlPO, and SiO₂).

Also, no apparent dependence of catalytic performance on the oxygen atom affinities of the supporting oxides was observed.

Single-atom cobalt catalysts on various supporting oxides were prepared using a previously published method with minor modifications.⁷ The bis(amido) complex Co[N(SiMe₃)₂]₂¹⁰ was employed as a precursor to introduce cobalt centers on the oxide surface by stirring a hexanes solution of the complex with a hexanes suspension of the appropriate oxide (Scheme 1). The resulting material was thoroughly washed with hexanes and then calcined at 300 °C in air to remove residual organic material. The inorganic nature of the catalyst samples was verified by carbon, hydrogen, and nitrogen elemental analyses

Scheme 1. Synthesis of Single-Atom Cobalts on Oxide Surfaces



Received: December 30, 2014

Revised: March 16, 2015

Published: March 16, 2015

(CHN values determined for all samples: C < 0.14, H < 0.90, N < 0.10).

The oxide support materials employed in this work (TiO₂, MgO, SBA-15, AlPO, and Y-Zeolite) were chosen to span a range of surface acidities and oxygen atom affinities. Surface acidities of the oxides were estimated by the solids' reported proton affinities,¹¹ and oxygen atom affinities were estimated by the E–O bond dissociation energies (E = Si, Al, P, Ti, and Mg; the average of both constituents was assumed for AlPO and Y-Zeolite).¹² Low precursor loadings were chosen for all samples to ensure the single-atom nature of the cobalt catalytic centers.⁷ Cobalt content in all samples was verified by inductively coupled plasma optical emission spectroscopy (ICP-OES). The synthesized samples of cobalt on MgO (CoMgO, 0.24 wt % Co), TiO₂ (CoTiO₂, 0.26 wt % Co), AlPO (CoAlPO, 0.22 wt % Co), SBA-15 (CoSBA, 0.27 wt % Co),¹³ and Y-Zeolite (CoYZ, 0.31 wt % Co) contained predominantly single-atom sites on the surface as evidenced by the extended X-ray absorption fine structure (EXAFS) spectra (Figures S1–S4). All of the samples' EXAFS spectra contain no significant peaks at apparent distances greater than 2.5 Å which indicates that second coordination shell interactions with neighboring cobalt atoms are negligible and suggests that most of the cobalt centers involve a single metal atom. The existence of dimeric cobalt units cannot be discounted without a complete modeling of the structure; however, the absence of features with intensity greater than 20% of that of the Co–O interaction at longer apparent distances (>2.5 Å) for all samples suggests that the degree of catalytic contribution from any dimeric units is similar for all samples in this comparative study. The Co–O distances were also similar for all samples (ca. 2.0 Å) and similar to those reported for molecular species.⁷ It is worth noting that based on the size of the molecular precursor used in this study, the cobalt sites in CoYZ are probably not within the zeolite channels.

As in CoSBA materials,⁷ the cobalt atoms in CoMgO, CoTiO₂, CoAlPO, and CoYZ are covalently bound to the surface via Co–O–E type linkages.¹⁴ The samples' IR spectra after grafting revealed a diminished intensity of the EO–H vibration¹⁵ at ca. 3580 cm⁻¹ and appearance of new Co–O–E vibrations (1090 cm⁻¹ for MgO, 1098 cm⁻¹ for AlPO, 980 cm⁻¹ for TiO₂, and 960 cm⁻¹ for YZ).¹⁴ UV–vis spectroscopy and X-ray absorption near edge structure (XANES) spectroscopy were employed to probe the oxidation states of the surface cobalt centers. The d–d transitions characteristic of the pseudotetrahedral Co²⁺ centers^{16,17} are found in the UV–vis spectra of CoYZ, CoTiO₂, CoSBA,¹³ and CoAlPO samples (ca. 550, 600, and 640 nm; Figures S5–S7). XANES spectra of these materials further confirm the +2 oxidation states of cobalt atoms with cobalt edge energies found at ca. 7719.5 eV (Figure 1).¹⁸ On the other hand, the UV–vis spectrum of CoMgO exhibits a peak at 430 nm (Figure S8), characteristic of Co³⁺ centers on an oxide.¹⁹ In addition, the XANES spectrum of CoMgO (Figure 1) displays an edge energy of ca. 7722 eV, which suggests that the overall oxidation state of the cobalt centers is between 2+ and 3+ (for comparison, the edge energy for Co^{II}Co^{III}₂O₄ is at ca. 7723 eV; Figure S9). All samples in this study contain a pre-edge feature in their XANES spectra at ca. 7709 eV (a 1s to 3d transition) that indicates the presence of noncentrosymmetric Co²⁺ centers, which is consistent with the aforementioned spectroscopic observations.

Photochemical water oxidation experiments were conducted employing CoMgO, CoTiO₂, CoAlPO, CoYZ, and CoSBA as catalysts. A buffered aqueous solution at pH 5.5–5.6

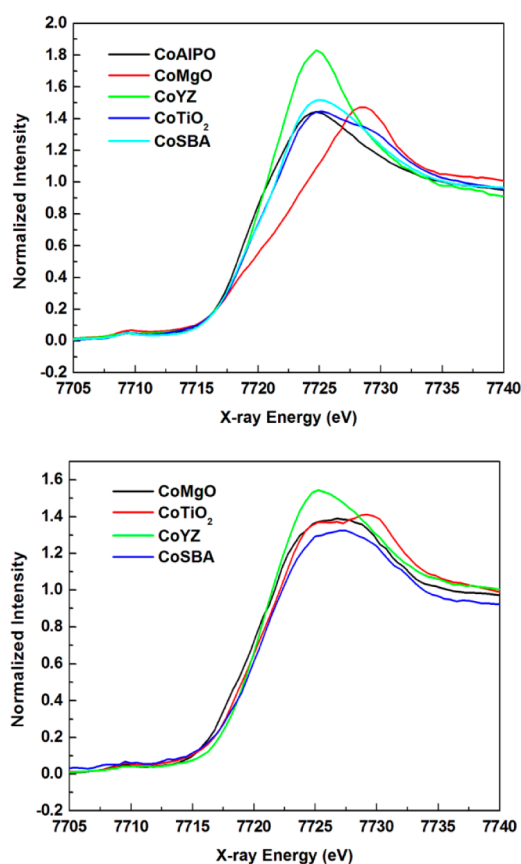


Figure 1. XANES spectra surface-bound cobalt catalysts (top). Notably, CoMgO exhibits a high edge energy compared to the other samples, indicating a higher average oxidation state. XANES spectra of the samples after catalysis are shown on the bottom. All of the samples reveal similar oxidation state (a mixture of 2+ and 3+) in their resting states. Postcatalysis XANES spectrum for CoAlPO was not collected due to the material's instability during catalysis.

(NaHCO₃/Na₂SiF₆) was used with Na₂S₂O₈ as a sacrificial electron acceptor and a [Ru(bpy)₃]Cl₂ sensitizer.⁴ A 488 nm laser with a power output of 260 mW and a focused beam diameter of 0.5 cm was selected as the light source. The headspace oxygen concentration was monitored in real-time using a fluorescence-based oxygen probe. The same amount of catalyst (40 mg) was used for each experiment. CoMgO, CoYZ, CoTiO₂, and CoSBA produced oxygen at good catalytic rates (Figure 2). Note that no oxygen evolution occurred in the absence of the [Ru(bpy)₃]Cl₂ sensitizer, suggesting that the oxidation of the catalyst by Ru³⁺ is a required step during catalysis as suggested by literature precedents (Figure S10).⁴ The active catalysts were recycled and achieved turnover numbers greater than 50 with additional portions of Na₂S₂O₈. No cobalt leaching was observed by ICP-OES after 25 turnovers. The CoAlPO material deactivated after ca. 3 turnovers as it decomposed and dissolved into solution. The generation of locally concentrated low pH sites during catalysis is likely responsible for the AlPO degradation.

The catalysts' initial turnover frequencies (TOF_i s) are also plotted in Figure 2.¹³ Notably, the TOF_i s of CoMgO and CoTiO₂ are 3 times greater than that of CoSBA and ca. 100 fold greater than that of a surface atom of a Co₃O₄ nanoparticle.⁷ Surface acidities of the supporting oxides appear to affect the TOF_i (Figure 3), as catalysis on more basic oxides

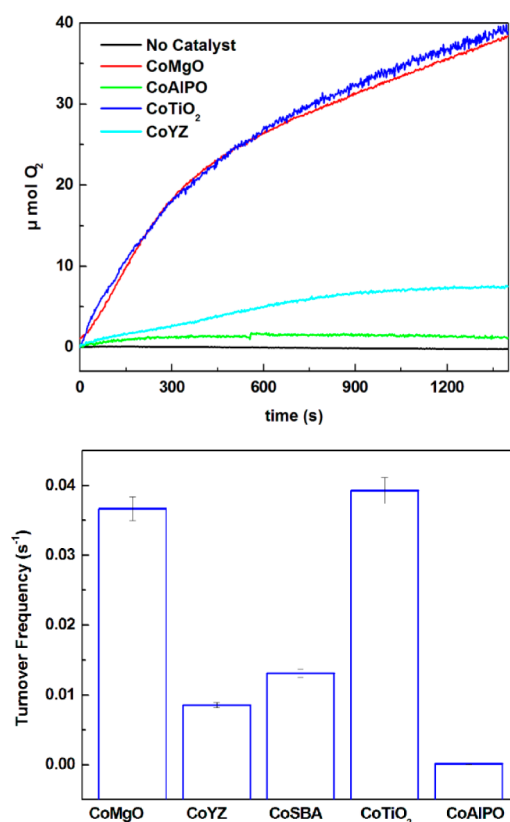


Figure 2. Oxygen evolution of surface-bound single-atom cobalt catalysts over time (top) and the initial turnover frequencies of the catalysts (bottom).

(MgO and TiO₂) exhibited catalytic rates significantly greater than those on acidic oxides (SBA-15 and Y-Zeolite).

Recent theoretical work by Mattioli and Guidoni suggests that the rate-determining step for oxygen evolution by a cobalt cluster involves the formation of a high-valent oxo, which then couples to a hydroxo or an aqua ligand on the same cobalt to generate the O–O bond.⁹ From this proposed mechanism, we hypothesized that for a single-atom cobalt catalyst bound to an oxide surface, the oxide's oxygen atom affinity may affect the rate of catalysis because it might dictate the rate of O–O bond formation and O₂ release. The oxygen atom affinities of the oxides employed in this work have been estimated by the E–O bond dissociation energies (E = Si, Al, P, Ti, and Mg; the average of both constituents was assumed for AlPO and Y-Zeolite).¹² The E–O bond dissociation energies were adopted from a calculation by Dumesic and co-workers based on known heats of formations of the oxides (for detailed calculations, see ref 12). However, a plot of the catalysis rates as a function of surface oxide oxygen atom affinities (Figure 3) revealed no apparent relationship between the TOF_i and the oxygen atom affinities of the supporting oxides. Presumably, the interaction of the oxygen atom with a neighboring E atom is not involved in the rate-limiting step of the catalysis.

The influence of redox-inactive metals (e.g., Ca and Zn) on the oxidation potential of redox-active metals (Mn and Fe) in synthetic mimics of photosystem II has recently been studied by Agapie and co-workers.^{20–23} The redox potentials of Mn and Fe in structurally analogous compounds shifted to >500 mV depending on the redox-inactive metal, suggesting significant electronic interactions between the redox-active and redox-inactive metals.^{20–23} A related analysis of the

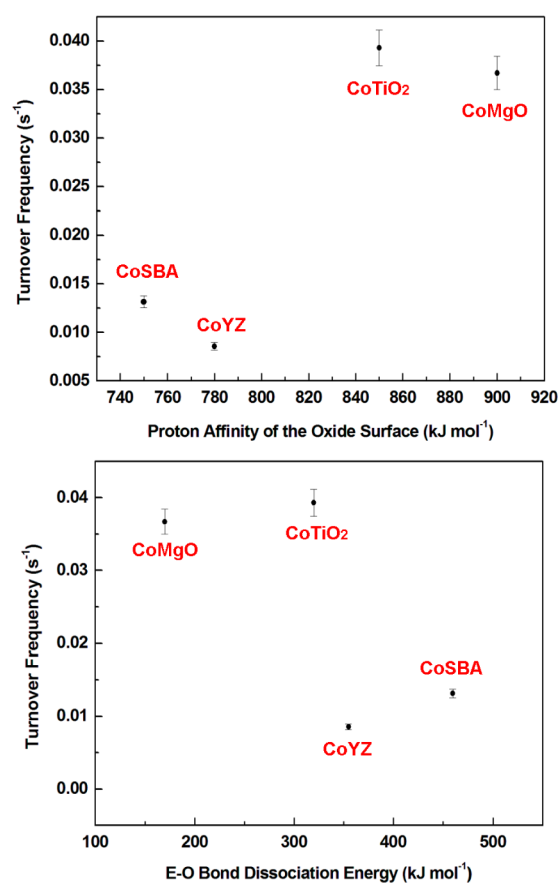


Figure 3. TOF_i s of the catalysts were plotted as functions of the properties of supporting oxides: surface acidity (top) and oxygen atom affinity (bottom). The data for CoAlPO was not included due to its instability during catalysis.

catalysts in this study was made by correlation of the TOF_i values to the Lewis acidities of E (Figure S11). A trend similar to that obtained with the TOF_i–proton affinity correlation was observed: cobalt on oxides of low Lewis acidity exhibited superior performance compared to those on oxides of high Lewis acidity. However, the distribution is bimodal, unlike the linear relationship observed between the Lewis acidities of redox-inactive atoms and the redox potential of the metals.^{21–23}

The cobalt centers' oxidation states were analyzed after catalysis by XANES spectroscopy (Figure 1). All of the catalytically active samples (CoSBA, CoTiO₂, CoMgO, and CoYZ) revealed a similar edge energy of ca. 7721 eV, lower than that of Co₃O₄ (7723.2 eV, Figure S9), suggesting that the ratio of Co²⁺ to Co³⁺ is lower than 1:2. The overall mixed Co²⁺–Co³⁺ oxidation state in these catalysts' resting states is consistent with many proposed mechanisms that suggest that the oxidation of Co²⁺ to Co³⁺ precedes the rate-determining step, which is believed to be a further oxidation of a Co³⁺ species.^{9,24} Notably, compared to the oxidation state before catalysis, the cobalt centers in CoMgO are overall reduced after catalysis, confirming that Co²⁺ is involved in the catalytic cycle.

In summary, a molecular method for introducing single-atom cobalt sites onto a supporting oxide has been expanded beyond silica to a variety of other oxide surfaces. Water oxidation catalysis by single-atom cobalt centers on various oxides was observed and quantified. Cobalt centers supported on basic oxides (MgO and TiO₂) exhibited superior catalytic performance compared to those on acidic oxides (Y-Zeolite and SiO₂).

A cobalt center on MgO exhibited a TOF_i of 0.04 s^{-1} , which is 3 times greater than that of a cobalt atom on SBA-15 and 100 times greater than that of a Co_3O_4 surface atom.⁷ Contrary to what might be expected based on theoretical work,⁹ no apparent correlation between the catalytic TOF_i and the oxygen atom affinities of the surface oxides was observed. XANES spectroscopy of the resting oxidation states of the catalysts revealed mixed oxidation states of Co^{2+} and Co^{3+} , which suggests that the rate-determining step requires a further oxidation of Co^{3+} , as proposed in many mechanistic models.^{9,20}

■ ASSOCIATED CONTENT

📎 Supporting Information

The following file is available free of charge on the ACS Publications website at DOI: 10.1021/cs502120f.

EXAFS and DRUV-vis spectra of CoAlPO , CoMgO , CoTiO_2 , and CoYZ samples ([PDF](#))

■ AUTHOR INFORMATION

Corresponding Author

*E-mail: tdtilley@berkeley.edu.

Present Address

†(H.S.A.) Center for Electrochemistry, Department of Chemistry, The University of Texas at Austin, Austin, Texas 78712, United States.

Notes

The authors declare no competing financial interest.

■ ACKNOWLEDGMENTS

This work was supported by the Director, Office of Science, Office of Basic Energy Sciences of the U.S. Department of Energy under contract no. DE-AC02-05CH11231. XAS data collection was carried out at the Advanced Light Source (ALS), which is supported by the Director, Office of Science, Office of Basic Energy Sciences (OBES), of the U.S. Department of Energy (DOE), under Contract No. DE-AC02-05CH11231. A part of the XAS data collection was also carried out at the Stanford Synchrotron Radiation Lightsource (SSRL) at BL 7.3, a Directorate of SLAC National Accelerator Laboratory and an Office of Science User Facility operated for the U.S. Department of Energy Office of Science by Stanford University. The SSRL Structural Molecular Biology Program is supported by the DOE Office of Biological and Environmental Research, and by the National Institutes of Health, National Institute of General Medical Sciences (including P41GM103393) and the National Center for Research Resources (P41RR001209).

■ REFERENCES

- (1) Gray, H. B. *Nat. Chem.* **2009**, *1*, 7.
- (2) Dau, H.; Christian, L.; Reier, T.; Risch, M.; Roggan, S.; Strasser, P. *ChemCatChem.* **2010**, *2*, 724–761.
- (3) Romain, S.; Vigara, L.; Llobet, A. *Acc. Chem. Res.* **2009**, *42*, 1944–1953.
- (4) Youngblood, W. J.; Lee, S.-H. A.; Maeda, K.; Mallouk, T. E. *Acc. Chem. Res.* **2009**, *42*, 1966–1973.
- (5) Surendranath, Y.; Kanan, M. W.; Nocera, D. G. *J. Am. Chem. Soc.* **2010**, *132*, 16501–16509.
- (6) Zhong, D. K.; Gamelin, D. R. *J. Am. Chem. Soc.* **2010**, *132*, 4202–4207.
- (7) Ahn, H. S.; Yano, J.; Tilley, T. D. *Energy Environ. Sci.* **2013**, *6*, 3080–3087.

- (8) Kent, C. A.; Concepcion, J. J.; Dares, C. J.; Torelli, D. A.; Rieth, A. J.; Miller, A. S.; Hoertz, P. G.; Meyer, T. J. *J. Am. Chem. Soc.* **2013**, *135*, 8432–8435.
- (9) Mattioli, G.; Giannozzi, P.; Bonapasta, A. A.; Guidoni, L. *J. Am. Chem. Soc.* **2013**, *135*, 15353–15363.
- (10) Burger, H.; Wannagat, U. *Monatsh. Chem.* **1963**, *94*, 1007.
- (11) Glazneva, T. S.; Kotsarenko, N. S.; Paukshtis, E. A. *Kinet. Catal.* **2008**, *49*, 859–867.
- (12) Rethwisch, D. G.; Dumesic, J. A. *Langmuir* **1986**, *2*, 73–79.
- (13) Note that the CoSBA data was adopted from a previously reported manuscript in ref 7.
- (14) Nakamoto, K. *Infrared and Raman Spectra of Inorganic and Coordination Compounds*; John Wiley & Sons, Inc: Hoboken, NJ, 2009.
- (15) Yoon, C. W.; Hirsekorn, K. F.; Neidig, M. L.; Yang, X.; Tilley, T. D. *ACS Catal.* **2011**, *1*, 1665–1678.
- (16) Taylor, C. M.; Watson, S. P.; Bryngelson, P. A.; Maroney, M. J. *Inorg. Chem.* **2003**, *42*, 312–320.
- (17) Goodgame, D. M. L.; Goodgame, M. *Inorg. Chem.* **1965**, *4*, 139–143.
- (18) Lim, S.; Ciuparu, D.; Pak, C.; Dobek, F.; Chen, Y.; Harding, D.; Pfefferle, L.; Haller, G. L. *J. Phys. Chem. B* **2003**, *107*, 11048–11056.
- (19) Takada, S.; Fujii, M.; Kohiki, S. *Nano Lett.* **2001**, *1*, 379–382.
- (20) Kanady, J. S.; Tsui, E. Y.; Day, M. W.; Agapie, T. *Science* **2011**, *333*, 733–736.
- (21) Tsui, E. Y.; Tran, R.; Yano, J.; Agapie, T. *Nat. Chem.* **2013**, *5*, 293–299.
- (22) Tsui, E. Y.; Agapie, T. *Proc. Natl. Acad. Sci. U. S. A.* **2013**, *110*, 10084–10088.
- (23) Herbert, D. E.; Lionetti, D.; Rittle, J.; Agapie, T. *J. Am. Chem. Soc.* **2013**, *135*, 19075–19078.
- (24) Brunschwig, B. S.; Chou, M. H.; Creutz, C.; Ghosh, P.; Sutin, N. *J. Am. Chem. Soc.* **1983**, *105*, 4832–4833.